HHS Public Access

Author manuscript

Eur J Radiol. Author manuscript; available in PMC 2017 November 01.

Published in final edited form as:

Eur J Radiol. 2016 November ; 85(11): 1934–1940. doi:10.1016/j.ejrad.2016.08.023.

Clinical and CT characteristics of surgically resected lung adenocarcinomas harboring *ALK* rearrangements or *EGFR* mutations

Hua Wang[a], **Matthew B. Schabath**[b], **Ying Liu**[a,c], **Ying Han**[d], **Qi Li**[e], **Robert J. Gillies**[#c,f], and **Zhaoxiang Ye**[#a]

[a]Department of Radiology, Tianjin Medical University Cancer Institute and Hospital, National Clinical Research Center of Cancer, Key Laboratory of Cancer Prevention and Therapy, Tianjin, China

[b]Department of Cancer Epidemiology, H. Lee Moffitt Cancer Center and Research Institute, Tampa, FL, USA

[c]Department of Cancer Imaging and Metabolism, H. Lee Moffitt Cancer Center and Research Institute, Tampa, FL, USA

[d]Department of Biotherapy, Tianjin Medical University Cancer Institute and Hospital, National Clinical Research Center of Cancer, Key Laboratory of Cancer Prevention and Therapy, Tianjin, China

[e]Department of Pathology; Tianjin Medical University Cancer Institute and Hospital, National Clinical Research Center of Cancer, Key Laboratory of Cancer Prevention and Therapy, Tianjin, China

[f]Department of Radiology; H. Lee Moffitt Cancer Center and Research Institute, Tampa, FL, USA

[#] These authors contributed equally to this work.

Abstract

Purpose—To determine if clinical and CT characteristics of surgically resected lung adenocarcinomas can distinguish those harboring *ALK* rearrangements from *EGFR* mutations.

Materials and Methods—Patients who had surgical resection and histologically confirmed lung adenocarcinoma were enrolled, including 41 patients with *ALK* rearrangements and 66 patients with *EGFR* mutations. Eighteen categorical and six quantitative CT characteristics were used to evaluate the tumors. Differences in clinical and CT characteristics between the two groups were investigated.

Corresponding Author: Zhaoxiang Ye, M.D., Tianjin Medical University Cancer Institute and Hospital, Huan-Hu-Xi Road, Ti-Yuan-Bei, He Xi District, Tianjin, 300060, PR China. Tel: +86-22-23536933; Fax: +86-22-23537796; yezhaoxiang@163.com.

Conflict of interest

All authors declare that they have no conflict of interest to declare.

Results—Age ($P = 0.003$), histological subtypes ($P < 0.001$), pathological stage ($P = 0.007$), and five CT characteristics, including size ($P < 0.001$), GGO ($P = 0.001$), bubble-like lucency ($P = 0.048$), lymphadenopathy ($P = 0.001$), and tumor shadow disappearance rate ($P = 0.005$) were significantly different between patients harboring *ALK* rearrangements compared to patients with *EGFR* mutations. When we compared histologic components, a solid pattern was more common ($P = 0.009$) in tumors with *ALK* rearrangements, and lepidic and acinar patterns were more common ($P < 0.001$ and $P = 0.040$, respectively) in those with *EGFR* mutations. Backward elimination analyses revealed that age (OR = 0.93; 95% CI 0.89 – 0.98), GGO (OR = 0.14; 95% CI 0.03 – 0.67), and lymphadenopathy (OR = 4.15; 95% CI 1.49 – 11.60) were significantly associated with *ALK* rearrangement status.

Conclusion—Our analyses revealed that clinical and CT characteristics of lung adenocarcinomas harboring *ALK* rearrangements were significantly different, compared with those with *EGFR* mutations. These differences may be related to the molecular pathology of these diseases.

Keywords

Computed tomography; *ALK*; *EGFR*; Lung adenocarcinoma; Histological subtype

1. Introduction

Over the last decade, advances in molecular testing have resulted in a paradigm shift whereby lung cancers are classified and treated based on genetic alternations that are critical to tumor growth and survival and can be exploited with targeted agents [1]. For example, the discovery that epidermal growth factor receptor (*EGFR*) mutations are effective targets for *EGFR* tyrosine kinase inhibitors (TKIs) has revolutionized therapeutic strategies [2]. More recently, the fusion oncogene of echinoderm microtubule-associated protein like 4 (*EML4*) and anaplastic lymphoma kinase (*ALK*) was newly identified in a subset of non-small cell lung cancer (NSCLC), primarily in lung adenocarcinoma [3]. *ALK* fusions occur in approximately 5% of lung adenocarcinoma, typically occur in a mutually exclusive manner to *EGFR* mutations [4-6], and *ALK* inhibitors, such as crizotinib, have been developed and tumors with *ALK* rearrangements have shown striking responses [7].

Pathologically and biologically, lung adenocarcinoma is a heterogeneous disease. Genetic heterogeneity has been identified not only between individual tumors of the same histopathologic subtype but also between primary lesions and associated metastatic sites in the same patient, and even between spatially separated regions within a single tumor [8, 9]. Hence, the tumor genomics landscape portrayed from single tumor biopsy samples obtained from primary or metastatic sites may be inaccurate and underestimated [8]. Sequential or multiple biopsies to identify subclones can rarely be implemented in routine clinical care because of logistical and financial barriers. Compared with molecular technologies, routine imaging provides a non-invasive and comprehensive view of the entire tumor and can be utilized to monitor tumor progression and therapy response, and potentially to identify locations for biopsy to provide the most actionable data.

To date there have been few published studies assessing the association between CT imaging features and *ALK* rearrangements among NSCLC patients [6, 10-16], and the results were still somewhat conflicting. Most of these studies included advanced tumors whose histology and mutational status were obtained from biopsy samples of primary or metastatic sites that may not accurately reflect the pathological and molecular characteristics of the tumor [10-15]. To identify characteristics that are associated with *ALK*-positive lung adenocarcinoma, this study compared clinical and CT characteristics between lung adenocarcinomas harboring *ALK* rearrangements versus those with *EGFR* mutations in a cohort of patients whose histopathologic and molecular diagnosis were confirmed by surgical resection.

2. Materials and Methods

2.1. Study population

The institutional review board of Tianjin Medical University approved this retrospective study. Written informed consent to undergo the pathological or gene mutational test was obtained from all patients beforehand.

We searched our database for those patients who had surgical resection for primary lung cancer and undergone both *ALK* fusion and *EGFR* mutation detection at our institution between January 2014 and July 2015. Inclusion criteria were those cases who had histologically confirmed lung adenocarcinoma with *ALK* rearrangements or *EGFR* mutations and available preoperative CT images on our picture archiving and communication system (PACS) performed less than 1 month before the subsequent surgery. Since the mutational rate of *EGFR* was much higher than that of *ALK* (20% to 50% for *EGFR* vs. 5% for *ALK*) in lung adenocarcinomas of Asian populations [6, 17], we then randomly selected 25% of those cases with *EGFR* mutations for comparison. Two cases underwent chemotherapy or radiotherapy before surgery and one case that harbored both mutations were excluded. Finally, 41 patients with *ALK* rearrangements and 66 patients with *EGFR* mutations were included in this study. For *EGFR* mutations, exon 21 mutation was most frequent (31/66, 47.0%), other mutations were located in exon 19, 20, or 18 (26, 8, and 3 cases, respectively).

2.2. Clinical and pathological characteristics

For each patient, age, gender, smoking status (never, former, and current smokers), preoperative serum carcinoembryonic antigen (CEA) level, histological subtypes and pathological TNM stage were extracted from patient medical records. Tumors were histologically classified according to the 2015 WHO classification, and each component was documented by making a semiquantitative estimate of all of the different histologic patterns present in 5% increments [18]. Tumors were pathologically staged according to the seventh edition of the Union for International Cancer Control and American Joint Committee on Cancer TNM classification system [19].

2.3. CT characteristics

Chest CT examinations were performed before surgery by using one of three multi-detector CT systems: Somatom Sensation 64 (Siemens Medical Solutions, Forchheim, Germany), Light speed 16, and Discovery CT750 HD (GE Healthcare, Milwaukee, WI, USA) scanner. Scanning parameters were as follows: 120 kVp with tube current adjusted automatically, 1.5 mm reconstruction thickness with 1.5 mm reconstruction interval for 64-detector scanner; and 120 kVp, 150–200 mA, 1.25 mm reconstruction thickness with 1.25 mm reconstruction interval for the other two scanners. Additional contrast-enhanced CT was performed for 96 patients. Non-ionic iodine contrast material (Ultravist, 300 mg of iodine per milliliter, Bayer Pharma, Berlin, Germany) was injected into the antecubital vein at a dose of 1.3-1.5ml per kilogram of body weight at a rate of 2.5 mL/sec by using an automated injector with a 70-second delay.

The images were reconstructed with high-resolution reconstruction algorithm for a pulmonary window setting (Width 1,200HU, Level −500HU) and with standard reconstruction algorithm for a mediastinal window setting (Width 320HU, Level 35HU).

Two radiologists with 9 and 6 years of experience in chest CT diagnosis independently reviewed all of the CT images on our PACS. Both radiologists were aware that patients had surgically resected lung adenocarcinomas but were unaware of the clinical data as well as the histological subtype or mutational status. As shown in Table 1, 18 characteristics were rated as categorical variables by assessing all slices and reporting with a standardized scoring sheet. Final conclusions were reached in consensus by discussion for discrepancy. The maximum dimension of the tumor (Dmax) and the largest dimension perpendicular to the maximum axis (Dper) on both pulmonary and mediastinal settings (pDmax, pDper, mDmax, and mDper) were measured and tumor shadow disappearance rate (TDR) was calculated. TDR was used to describe the GGO ratio of the tumor, and was regarded as a criterion for evaluating radiological invasiveness of lung cancer. TDR was calculated using the following formula: TDR = 1 − (mDmax × mDper/pDmax × pDper) [6]. CT attenuation value was measured by placing a region of interest (ROI) as large as possible and avoiding the air-containing space within the confine of the tumor. The degree of contrast enhancement was calculated by subtracting the CT value of pre-contrast from that of post-contrast for those patients performed contrast-enhanced CT scanning.

2.4. Statistical analyses

Statistical analyses were performed by using Stata/MP 14.1 (StataCorp LP, College Station, TX). To compare patients with *EGFR* mutant tumors versus patients with *ALK* positive tumors, Fisher's exact test was used for categorical variables and Student's t test was used for continuous variables. Multivariable logistic regression analysis was used to generate odds ratios (ORs) and 95% confidence intervals (CIs). The dependent variable was mutational status (*EGFR* mutation versus *ALK* positivity) and the clinical and CT characteristics were the independent features. Backward elimination analyses were used to select the most informative variables into a single parsimonious model. The clinical and CT characteristic that was statistically significant was considered for inclusion into the backward elimination analyses. A *P* value of less than 0.05 was considered statistically significant.

3. Results

3.1. Clinical and pathological characteristics

The distribution of the clinical and pathological characteristics by mutational status is presented in Table 2. Patients with *ALK* rearrangements (54.8 years ± 9.1) were significantly younger ($P = 0.003$) than those with *EGFR* mutations (60.2 years ± 8.7). No significant differences were found in gender, smoking status, and preoperative CEA level between the two groups. There were significant differences in histologic subtypes between the two groups ($P < 0.001$). Specifically, a solid adenocarcinoma pattern was more common ($P = 0.009$) in adenocarcinomas with *ALK* rearrangements (n = 20, 48.8%) than in those with *EGFR* mutations (n = 16, 24.2%), and lepidic and acinar patterns were more common ($P < 0.001$ and $P = 0.040$, respectively) in adenocarcinomas with *EGFR* mutations (n = 41, 62.1% and n = 51, 77.3%, respectively) than in those with *ALK* rearrangements (n = 4, 9.8% and n = 24, 58.5%, respectively). Pathological stage was significantly different between the two groups ($P = 0.007$). Specifically, there were more stage I tumors ($P = 0.002$) harboring an *EGFR* mutation (n = 33, 50.0%) than in those with *ALK* rearrangements (n = 8, 19.5%).

3.2. CT characteristics

The distribution of CT characteristics is presented in Table 3 and examples of CT images for each scale of categorical characteristics are shown in Figure S1. Size ($P < 0.001$), ground-glass opacity (GGO) ($P = 0.001$), bubble-like lucency ($P = 0.048$), lymphadenopathy ($P = 0.001$), and tumor shadow disappearance rate ($P = 0.005$) were significant different between lung adenocarcinomas harboring *ALK* rearrangements versus those with *EGFR* mutations. Specifically, tumors greater than 5 cm were found more frequently ($P = 0.001$) in adenocarcinomas with *ALK* rearrangements (n = 13, 31.7%) than in those with *EGFR* mutations (n = 5, 7.6%). GGO and bubble-like lucency ($P = 0.001$ and $P = 0.022$, respectively) were more common in adenocarcinomas with *EGFR* mutations (n = 22, 33.3% and n = 23, 34.8%, respectively) than in those with *ALK* rearrangements (n = 2, 4.9% and n = 6, 14.6%, respectively) (Figure 1). As a quantitative index to describe GGO, the TDR was larger ($P = 0.005$) in adenocarcinomas with *EGFR* mutations (0.21 ± 0.24) than in those with *ALK* rearrangements (0.09 ± 0.09). Lymphadenopathy was more common ($P = 0.001$) in adenocarcinomas with *ALK* rearrangements (n = 23, 56.1%) than in those with *EGFR* mutations (n = 16, 24.2%), and furthermore, lymphadenopathy present in N2 or N3 area was more common ($P < 0.001$) in adenocarcinomas with *ALK* rearrangements (n = 18, 43.9%) than in those with *EGFR* mutations (n = 8, 12.1%) (Figure 2). Notably, necrosis was found in 3 adenocarcinomas with *ALK* rearrangements (7.3%), while none with *EGFR* mutations presented with necrosis. No significant differences between CT values of pre-contrast, post-contrast or the degree of contrast enhancement were found between the two groups.

We utilized a backward elimination approach to generate a single parsimonious model of the most informative covariates. All covariates that were found to be statistically significantly different in Tables 2 and 3 were considered for the inclusion. The final model included only three covariates: age, GGO, and lymphadenopathy. Based on the backward elimination approach, lymphadenopathy categorized as absent and present with enlarged lymph nodes in N1 area only were determined to be a referent group. Age (OR = 0.93; 95% CI 0.89 – 0.98)

and GGO (OR = 0.14; 95% CI 0.03 – 0.67) were inversely associated with *ALK* rearrangement status while lymphadenopathy (OR = 4.15; 95% CI 1.49 – 11.60) was directly associated with *ALK* rearrangement status (Table 4).

4. Discussion

In this study we investigated the differences in clinical and CT characteristics between lung adenocarcinomas harboring *ALK* rearrangements and those with *EGFR* mutations in 107 patients treated by surgical resection. Backward elimination analyses revealed that age, GGO, and lymphadenopathy were significantly associated with *ALK* rearrangement status. Patients with *ALK* rearrangements were younger, and were more likely to have CT characteristics of solid pattern and lymphadenopathy of N2 or N3 area than those with *EGFR* mutations.

The distinction between *ALK*-rearranged and *EGFR*-mutated lung adenocarcinomas is important because *ALK*-rearranged tumors are strongly associated with resistance to *EGFR* TKIs [20], and more importantly, the *ALK* inhibitors have shown striking responses in *ALK*-rearranged NSCLC, and have been approved for the standard treatment of *ALK*-positive NSCLC in many countries. The clinical features of patients with *ALK*-rearranged lung adenocarcinomas have been reported to be similar to those with *EGFR* mutations, such as younger age and never or light smokers [4-6]. *ALK*-rearranged patients were observed even younger than the *EGFR*-mutated population [10, 21]. The age was the only preoperative clinical characteristic which was significantly different between the two groups in our study. However, because of the tremendous overlap, it's hard to discriminate the two mutations using the age alone.

Previous studies have shown that *ALK*-rearranged lung adenocarcinomas were significantly associated with solid predominant subtype [22] and *EGFR*-mutated tumors were significantly associated with lepidic predominant subtype [23]. However, lung adenocarcinomas frequently are composed of complex heterogeneous mixtures of patterns with a continuum from one pattern to the next. In the 2015 WHO classification, the term “predominant” is not listed in the name for the major adenocarcinoma subtypes as it was in the 2011 IASLC/ATS/ERS lung adenocarcinoma classification [18]. Therefore, any analyses based on a pathologic diagnosis of the predominant component in lung adenocarcinoma may not adequately determine the pathologic features of *ALK* rearrangements. We explored the association between each component and mutational status, and found a solid pattern was more common ($P = 0.009$) in adenocarcinomas with *ALK* arrangements, and lepidic and acinar patterns were more common ($P < 0.001$ and $P = 0.040$, respectively) in those with *EGFR* mutations. However, because of the intratumoral heterogeneity on the histologic features of lung adenocarcinoma, these features cannot be completely detected by single biopsies before surgery, and also, it's not enough to discriminate the two mutations through histologic features alone even using the resection specimens.

Radiogenomics, focused on defining relationships between image features (or “image phenotypes”) and molecular markers (or “molecular phenotypes”), is an emerging field for extending clinical imaging into the era of molecular imaging [24]. In a recent study, we have

shown CT features associated with *EGFR*-mutated lung adenocarcinomas [25]. In this present study, we investigated the abilities of CT findings to discriminate between the two actionable mutations in an independent population. Previous studies have attempted to assess CT characteristics associated with *ALK*-rearranged NSCLC. These studies revealed that *ALK*-rearranged tumors were more likely to be solid tumors without GGO and tumors with lower TDR [6, 14, 16]. Our results were consistent with these previous reports. Since it was generally recognized that adenocarcinomas showing GGO on CT usually possess lepidic growth pattern [26], the result is also consistent with the pathologic findings that lepidic growth pattern was more common in lung adenocarcinomas with *EGFR* mutations than in those with *ALK* rearrangements. By comparing with those with *EGFR* mutations, lung adenocarcinomas with *ALK* rearrangements were reported to be associated with advanced lymph node metastasis [10, 13]. In the present study on surgically resected lung adenocarcinomas, we found that lymphadenopathy present in N2 or N3 area and also the presence of lymphadenopathy was more common in adenocarcinomas with *ALK* rearrangements than in those with *EGFR* mutations. Although lymphadenopathy in our study is just a CT descriptor of the lymph nodes with a short axis of at least 10 mm, not necessarily means the pathologic metastasis of lymph nodes, this simple feature was also found to be significant in discriminate the two mutations.

While Choi *et al.* [10] and Kim *et al.* [16] found NSCLC with *ALK* rearrangements had lobulated margins, Zhou *et al.* [14] found lobulated margins were less frequently in lung adenocarcinomas with *ALK* rearrangements than in those with *EGFR* mutations. We did not detect a significant association between lobulation and *EGFR* or *ALK* status even using three categories to describe this characteristic in this cohort of resectable tumors with relatively early stage. Unlike the results from Kim *et al.* [16], we did not find difference in contrast enhancement between tumors harboring *ALK* rearrangements and those with *EGFR* mutations. The discrepancy in findings is likely due to differences in patient selection. The patients in Choi *et al.*'s study were advanced lung adenocarcinomas, the patients in Kim *et al.*'s study were surgically resected NSCLC, while Zhou *et al.* studied all stages of adenocarcinomas. We only studied lung adenocarcinomas confirmed by surgical resection, and compared the histological difference between tumors with the two mutations using the new 2015 WHO classification to further investigate the pathological basis of the imaging characteristics.

We acknowledge that there are some limitations in the present study. First, the sample size of our study was relatively small. Because of the low incidence of *ALK* rearrangements, large multi-institutional studies are needed to confirm our findings. Next, to avoid the sampling artifacts and interference of treatment, we only analyzed surgically resected lung adenocarcinomas to get the exact pathologic and molecular diagnosis, and imaging features before any treatments. However, whether the results apply to advanced-stage tumors needs to be assessed further. And since stage would potentially affect the clinical and imaging characteristics of cancer, further comparison with matched TNM staging should be performed in the future. Also, given the potential impact of genetic intratumoral heterogeneity on the histologic features of *ALK* fusions, the relationship between histologic subtype and mutational status may be more complex than we found. For the same reason, quantitative imaging features should be developed to measure the intratumoral heterogeneity

and to further predict genetic mutations. Additionally, PET-CT is useful in preoperative staging for lung cancer. However, we didn't include that information in this study because some of the cases didn't perform PET-CT before surgery.

In conclusion, patients with lung adenocarcinoma harboring *ALK* rearrangements appeared to have younger age and CT characteristics of solid pattern and more distant lymphadenopathy compared with those with *EGFR* mutations. This work may be helpful for guiding biopsy for specific gene mutational test, or treatment in the absence of mutational analyses. For example, we may obtain biopsy from the solid portion of the tumor with predominantly solid component to increase the possibilities of detection of *ALK* rearrangements in the younger patients with relatively distant thoracic lymphadenopathy.

Supplementary Material

Refer to Web version on PubMed Central for supplementary material.

Acknowledgments

Funding

This research was supported by National Natural Science Foundation of China (grant 81601492), Tianjin Science and Technology Major Project (grant 12ZCDZSY15500) and Public science and technology research funds projects of NHFPC of the P.R. China (grant 201402013), and by U.S. National Institutes of Health (grant U01 CA143062).

Role of the Funding Source:

The funders had no role in study design, the collection, analysis or interpretation of data, the writing of the paper, or the decision to submit.

Abbreviations

EGFR	epidermal growth factor receptor
ALK	anaplastic lymphoma kinase
TKIs	tyrosine kinase inhibitors
NSCLC	non-small cell lung cancer
PACS	picture archiving and communication system
CEA	serum carcinoembryonic antigen
TDR	tumor shadow disappearance rate
GGO	ground-glass opacity
OR	odds ratio
CI	confidence interval

References

1. Pao W, Girard N. New driver mutations in non-small-cell lung cancer. The lancet oncology. 2011; 12(2):175–80. [PubMed: 21277552]
2. Mok TS, Wu YL, Thongprasert S, Yang CH, Chu DT, Saijo N, Sunpaweravong P, Han B, Margono B, Ichinose Y, Nishiwaki Y, Ohe Y, Yang JJ, Chewaskulyong B, Jiang H, Duffield EL, Watkins CL, Armour AA, Fukuoka M. Gefitinib or carboplatin-paclitaxel in pulmonary adenocarcinoma. The New England journal of medicine. 2009; 361(10):947–57. [PubMed: 19692680]
3. Soda M, Choi YL, Enomoto M, Takada S, Yamashita Y, Ishikawa S, Fujiwara S, Watanabe H, Kurashina K, Hatanaka H, Bando M, Ohno S, Ishikawa Y, Aburatani H, Niki T, Sohara Y, Sugiyama Y, Mano H. Identification of the transforming EML4-ALK fusion gene in non-small-cell lung cancer. Nature. 2007; 448(7153):561–6. [PubMed: 17625570]
4. Camidge DR, Kono SA, Flacco A, Tan AC, Doebele RC, Zhou Q, Crino L, Franklin WA, Varella-Garcia M. Optimizing the detection of lung cancer patients harboring anaplastic lymphoma kinase (ALK) gene rearrangements potentially suitable for ALK inhibitor treatment. Clin Cancer Res. 2010; 16(22):5581–90. [PubMed: 21062932]
5. Wong DW, Leung EL, So KK, Tam IY, Sihoe AD, Cheng LC, Ho KK, Au JS, Chung LP, Pik Wong M. The EML4-ALK fusion gene is involved in various histologic types of lung cancers from nonsmokers with wild-type EGFR and KRAS. Cancer. 2009; 115(8):1723–33. [PubMed: 19170230]
6. Fukui T, Yatabe Y, Kobayashi Y, Tomizawa K, Ito S, Hatooka S, Matsuo K, Mitsudomi T. Clinicoradiologic characteristics of patients with lung adenocarcinoma harboring EML4-ALK fusion oncogene. Lung Cancer. 2012; 77(2):319–25. [PubMed: 22483782]
7. Shaw AT, Kim DW, Nakagawa K, Seto T, Crino L, Ahn MJ, De Pas T, Besse B, Solomon BJ, Blackhall F, Wu YL, Thomas M, O'Byrne KJ, Moro-Sibilot D, Camidge DR, Mok T, Hirsh V, Riely GJ, Iyer S, Tassell V, Polli A, Wilner KD, Janne PA. Crizotinib versus chemotherapy in advanced ALK-positive lung cancer. The New England journal of medicine. 2013; 368(25):2385–94. [PubMed: 23724913]
8. Gerlinger M, Rowan AJ, Horswell S, Larkin J, Endesfelder D, Gronroos E, Martinez P, Matthews N, Stewart A, Tarpey P, Varela I, Phillimore B, Begum S, McDonald NQ, Butler A, Jones D, Raine K, Latimer C, Santos CR, Nohadani M, Eklund AC, Spencer-Dene B, Clark G, Pickering L, Stamp G, Gore M, Szallasi Z, Downward J, Futreal PA, Swanton C. Intratumor heterogeneity and branched evolution revealed by multiregion sequencing. The New England journal of medicine. 2012; 366(10):883–92. [PubMed: 22397650]
9. Cai W, Lin D, Wu C, Li X, Zhao C, Zheng L, Chuai S, Fei K, Zhou C, Hirsch FR. Intratumoral Heterogeneity of ALK-Rearranged and ALK/EGFR Coaltered Lung Adenocarcinoma. J Clin Oncol. 2015; 33(32):3701–9. [PubMed: 26416997]
10. Choi CM, Kim MY, Hwang HJ, Lee JB, Kim WS. Advanced adenocarcinoma of the lung: comparison of CT characteristics of patients with anaplastic lymphoma kinase gene rearrangement and those with epidermal growth factor receptor mutation. Radiology. 2015; 275(1):272–9. [PubMed: 25575117]
11. Yamamoto S, Korn RL, Oklu R, Migdal C, Gotway MB, Weiss GJ, Iafrate AJ, Kim DW, Kuo MD. ALK molecular phenotype in non-small cell lung cancer: CT radiogenomic characterization. Radiology. 2014; 272(2):568–76. [PubMed: 24885982]
12. Park J, Yamaura H, Yatabe Y, Hosoda W, Kondo C, Shimizu J, Horio Y, Yoshida K, Tanaka K, Oguri T, Kobayashi Y, Hida T. Anaplastic lymphoma kinase gene rearrangements in patients with advanced-stage non-small-cell lung cancer: CT characteristics and response to chemotherapy. Cancer Med. 2014; 3(1):118–23. [PubMed: 24403104]
13. Halpenny DF, Riely GJ, Hayes S, Yu H, Zheng J, Moskowitz CS, Ginsberg MS. Are there imaging characteristics associated with lung adenocarcinomas harboring ALK rearrangements? Lung Cancer. 2014; 86(2):190–4. [PubMed: 25312988]
14. Zhou JY, Zheng J, Yu ZF, Xiao WB, Zhao J, Sun K, Wang B, Chen X, Jiang LN, Ding W. Comparative analysis of clinicoradiologic characteristics of lung adenocarcinomas with ALK rearrangements or EGFR mutations. Eur Radiol. 2015; 25(5):1257–66. [PubMed: 25577516]
15. Rizzo S, Petrella F, Buscarino V, De Maria F, Raimondi S, Barberis M, Fumagalli C, Spitaleri G, Rampinelli C, De Marinis F, Spaggiari L, Bellomi M. CT Radiogenomic Characterization of

EGFR, K-RAS, and ALK Mutations in Non-Small Cell Lung Cancer. Eur Radiol. 2016; 26(1):32–42. [PubMed: 25956936]

16. Kim TJ, Lee CT, Jheon SH, Park JS, Chung JH. Radiologic Characteristics of Surgically Resected Non-Small Cell Lung Cancer With ALK Rearrangement or EGFR Mutations. The Annals of thoracic surgery. 2016; 101(2):473–80. [PubMed: 26454747]
17. Woo T, Okudela K, Yazawa T, Wada N, Ogawa N, Ishiwa N, Tajiri M, Rino Y, Kitamura H, Masuda M. Prognostic value of KRAS mutations and Ki-67 expression in stage I lung adenocarcinomas. Lung Cancer. 2009; 65(3):355–62. [PubMed: 19162366]
18. Travis WD, Brambilla E, Nicholson AG, Yatabe Y, Austin JH, Beasley MB, Chirieac LR, Dacic S, Duhig E, Flieder DB, Geisinger K, Hirsch FR, Ishikawa Y, Kerr KM, Noguchi M, Pelosi G, Powell CA, Tsao MS, Wistuba I. The 2015 World Health Organization Classification of Lung Tumors: Impact of Genetic, Clinical and Radiologic Advances Since the 2004 Classification. J Thorac Oncol. 2015; 10(9):1243–60. [PubMed: 26291008]
19. Mirsadraee S, Oswal D, Alizadeh Y, Caulo A, van Beek E Jr. The 7th lung cancer TNM classification and staging system: Review of the changes and implications. World J Radiol. 2012; 4(4):128–34. [PubMed: 22590666]
20. Shaw AT, Yeap BY, Mino-Kenudson M, Digumarthy SR, Costa DB, Heist RS, Solomon B, Stubbs H, Admane S, McDermott U, Settleman J, Kobayashi S, Mark EJ, Rodig SJ, Chirieac LR, Kwak EL, Lynch TJ, Iafrate AJ. Clinical features and outcome of patients with non-small-cell lung cancer who harbor EML4-ALK. J Clin Oncol. 2009; 27(26):4247–53. [PubMed: 19667264]
21. Kim H, Jang SJ, Chung DH, Yoo SB, Sun P, Jin Y, Nam KH, Paik JH, Chung JH. A comprehensive comparative analysis of the histomorphological features of ALK-rearranged lung adenocarcinoma based on driver oncogene mutations: frequent expression of epithelial-mesenchymal transition markers than other genotype. PloS one. 2013; 8(10):e76999. [PubMed: 24194854]
22. Kim H, Chung JH. Overview of clinicopathologic features of ALK-rearranged lung adenocarcinoma and current diagnostic testing for ALK rearrangement. Transl Lung Cancer Res. 2015; 4(2):149–55. [PubMed: 25870797]
23. Villa C, Cagle PT, Johnson M, Patel JD, Yeldandi AV, Raj R, DeCamp MM, Raparia K. Correlation of EGFR mutation status with predominant histologic subtype of adenocarcinoma according to the new lung adenocarcinoma classification of the International Association for the Study of Lung Cancer/American Thoracic Society/European Respiratory Society. Archives of pathology & laboratory medicine. 2014; 138(10):1353–7. [PubMed: 24571650]
24. Kuo MD, Jamshidi N. Behind the numbers: decoding molecular phenotypes with radiogenomics-guiding principles and technical considerations. Radiology. 2014; 270(2):320–5. [PubMed: 24471381]
25. Liu Y, Kim J, Qu F, Liu S, Wang H, Balagurunathan Y, Ye Z, Gillies RJ. CT Features Associated with Epidermal Growth Factor Receptor Mutation Status in Patients with Lung Adenocarcinoma. Radiology. 2016; 280(1):271–80. [PubMed: 26937803]
26. Wang H, Schabath MB, Liu Y, Berglund AE, Bloom GC, Kim J, Stringfield O, Eikman EA, Klippenstein DL, Heine JJ, Eschrich SA, Ye Z, Gillies RJ. Semiquantitative Computed Tomography Characteristics for Lung Adenocarcinoma and Their Association With Lung Cancer Survival. Clinical lung cancer. 2015; 16(6):141–63.

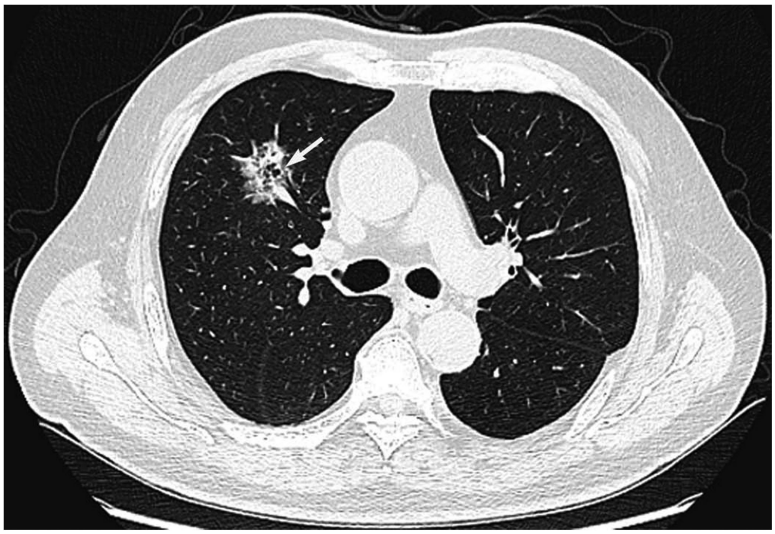

Figure 1.
CT image of a 70-year-old man with a lepidic adenocarcinoma harboring *EGFR* mutation shows a subsolid tumor with bubble-like lucency (arrow).

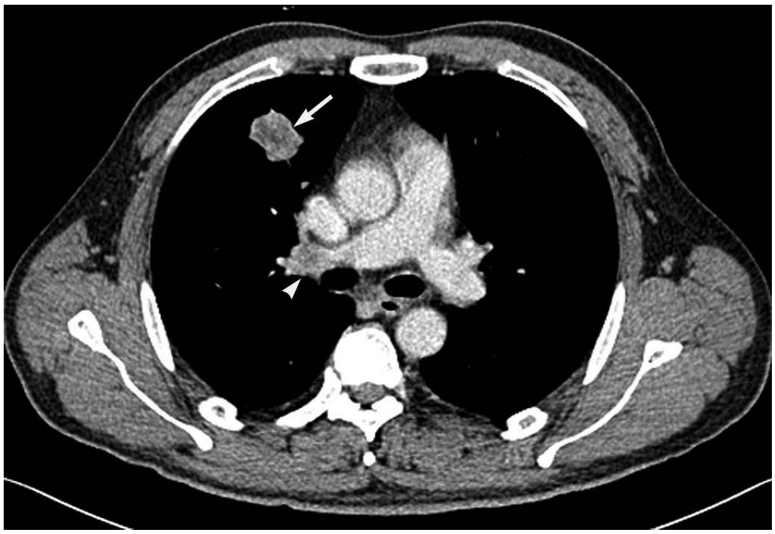

Figure 2.
CT image of a 47-year-old man with a solid adenocarcinoma harboring *ALK* rearrangement shows a solid tumor (arrow) with lymphadenopathy (arrowhead).

Table 1

Categorical CT characteristics for lung adenocarcinomas

Characteristic	Definition	Scoring	Scoring definition
Location	Central: involving segmental or more proximal bronchi; Peripheral: involving subsegmental bronchi or more distal airway	1,2	1. Central; 2. Peripheral
Size	The maximum dimension of the tumor in lung window	1,2,3,4,5	1. ≤2 cm; 2. >2-3 cm; 3. >3-5 cm; 4. >5-7 cm; 5. >7 cm
Pleural attachment	Tumor's margin obscured by the pleura or fissure	1,2,3	1. Absent; 2. Present but without mediastinal attachment; 3. Present and with mediastinal attachment
Pleural retraction	Retraction of the pleura toward the tumor with linear structure originating from the tumor and extending to the pleural surface	1,2	1. Absent; 2. Present
Lobulation	A portion of the surface of a lesion showing a shallow, wavy configuration, with the exception of the regions abutting the pleura	1,2,3	1. Absent; 2. Slight; 3. Obvious: at least three undulations with a height of more than 2 mm
Spiculation	The presence of linear strands extending from the nodule or mass margin into the lung parenchyma without reaching the pleural surface	1,2,3	1. Absent; 2. Fine; 3. Coarse: at least 2 mm thick
Concavity	V-shaped indentation of the border deeper than 3 mm	1,2	1. Absent; 2. Present
GGO	Hazy increased opacity of lung, with preservation of bronchial and vascular margins	1,2	1. Absent (solid); 2. Present (subsolid)
Air bronchogram	Air-filled bronchi seen as radiolucent, branching bands within tumor	1,2,3	1. Absent; 2. Small extent; 3. Large extent
Bubble-like lucency	Spots of air attenuation within tumor	1,2,3	1. Absent; 2. Small extent; 3. Large extent
Necrosis	Hypodense area of liquefaction in the tumor	1,2	1. Absent; 2. Present
Calcification	Any patterns of calcification in the tumor	1,2	1. Absent; 2. Present
Obstructive changes	Obstructive inflammation or atelectasis	1,2,3	1. Absent; 2. Slight; 3. Obvious
Involved vessel pattern	The pattern of vessels involved, only applied to the contrast-enhanced images	1,2,3	1. Into the tumor; 2. Around the tumor; 3. Passing through the tumor
Nodules in the same lobe	Indeterminate same lobe nodules with a long axis larger than 4mm	1,2	1. Absent; 2. Present
Nodules in other lobes	Indeterminate other lobe nodules with a long axis larger than 4mm	1,2	1. Absent; 2. Present
Lymphadenopathy	The presence of thoracic lymph nodes with a short axis of at least 10 mm	1,2,3	1. Absent; 2. Present with enlarged lymph nodes in N1 area only; 3. Present with enlarged lymph nodes in N2 or N3 areas[1]
Pleural nodules	Pleural nodules suspected metastases	1,2	1. Absent; 2. Present

Abbreviation: GGO, ground-glass opacity

[1] N1 area: enlargement in ipsilateral peribronchial and/or ipsilateral hilar lymph nodes and intrapulmonary nodes, including involvement by directly extension; N2 area: enlargement in ipsilateral mediastinal and/or subcarinal lymph nodes; N3 area: enlargement in contralateral mediastinal, contralateral hilar, ipsilateral or contralateral scalene, or supraclavicular lymph nodes

Table 2

Clinical and pathological characteristics of patients with an *EGFR* mutant tumor versus patients with an *ALK* positive tumor

Characteristic	*EGFR+*	*ALK+*	*P*-value
Gender, N (%)			
Female	46 (69.7)	23 (56.1)	
Male	20 (30.3)	18 (43.9)	0.212
Smoking status, N (%)			
Never	48 (72.7)	26 (63.4)	
Former	6 (9.1)	5 (12.2)	
Current	12 (18.2)	10 (24.4)	0.601
Mean age, (SD)	60.2 (8.7)	54.8 (9.1)	**0.003**
Mean CEA (ug/l), (SD)	14.4 (28.5)	10.3 (27.4)	0.462
Histology, N (%)			
MIA	1 (1.5)	0 (0.0)	
Lepidic adenocarcinoma	18 (27.3)	1 (2.4)	
Acinar adenocarcinoma	30 (45.5)	15 (36.6)	
Papillary adenocarcinoma	6 (9.1)	2 (4.9)	
Micropapillary adenocarcinoma	2 (3.0)	2 (4.9)	
Solid adenocarcinoma	7 (10.6)	16 (39.0)	
IMA	2 (3.0)	5 (12.2)	< **0.001**
Lepidic, N (%)			
absent	25 (37.9)	37 (90.2)	
present	41 (62.1)	4 (9.8)	< **0.001**
Acinar, N (%)			
absent	15 (22.7)	17 (41.5)	
present	51 (77.3)	24 (58.5)	**0.040**
Papillary, N (%)			
absent	52 (78.8)	35 (85.4)	
present	14 (21.2)	6 (14.6)	0.396
Micropapillary, N (%)			
absent	28 (42.4)	23 (56.1)	
present	38 (57.6)	18 (43.9)	0.169
Solid, N (%)			
absent	50 (75.8)	21 (51.2)	
present	16 (24.2)	20 (48.8)	**0.009**
Mucinous, N (%)			
absent	59 (89.4)	36 (87.8)	
present	7 (10.6)	5 (12.2)	1.000
Pathological stage, N (%)			
Ia	20 (30.3)	6 (14.6)	
Ib	13 (19.7)	2 (4.9)	

Characteristic	*EGFR+*	*ALK+*	*P*-value
IIa	6 (9.1)	8 (19.5)	
IIb	0 (0.0)	1 (2.4)	
IIIa	19 (28.8)	15 (36.6)	
IIIb	2 (3.0)	6 (14.6)	
IV	6 (9.1)	3 (7.3)	**0.007**[1]

Abbreviations: MIA, minimally invasive adenocarcinoma; IMA, invasive mucinous adenocarcinoma

Bolded values indicate a statistically significant result

[1] *P* value was derived by combing Ia and Ib, IIa and IIb, and IIIa and IIIb

Table 3

CT characteristics of patients with an *EGFR* mutant tumor versus patients with an *ALK* positive tumor

Characteristic	*EGFR+*	*ALK+*	*P*-value
Location, N (%)			
1	12 (18.2)	14 (34.1)	
2	54 (81.8)	27 (65.9)	0.069
Size, N (%)			
1	6 (9.1)	8 (19.5)	
2	24 (36.4)	13 (31.7)	
3	31 (46.9)	7 (17.1)	
4	5 (7.6)	9 (21.9)	
5	0 (0.0)	4 (9.8)	< **0.001**
Pleural attachment, N (%)			
1	22 (33.3)	9 (22.0)	
2	27 (40.9)	14 (34.1)	
3	17 (25.8)	18 (43.9)	0.149
Pleural retraction, N (%)			
1	2 (3.0)	5 (12.2)	
2	64 (97.0)	36 (87.8)	0.104
Lobulation, N (%)			
1	3 (4.6)	3 (7.3)	
2	29 (43.9)	16 (39.0)	
3	34 (51.5)	22 (53.7)	0.764
Spiculation, N (%)			
1	12 (18.2)	9 (21.9)	
2	22 (33.3)	20 (48.8)	
3	32 (48.5)	12 (29.3)	0.141
Concavity, N (%)			
1	15 (22.7)	16 (39.0)	
2	51 (77.3)	25 (61.0)	0.083
GGO, N (%)			
1	44 (66.7)	39 (95.1)	
2	22 (33.3)	2 (4.9)	**0.001**
Airbronchogram, N (%)			
1	22 (33.3)	20 (48.8)	
2	29 (43.9)	18 (43.9)	
3	15 (22.7)	3 (7.3)	0.073
Bubble-like lucency, N (%)			
1	43 (65.2)	35 (85.4)	
2	17 (25.8)	3 (7.3)	
3	6 (9.1)	3 (7.3)	**0.048**
Necrosis, N (%)			

Characteristic	*EGFR+*	*ALK+*	*P*-value
1	66 (100.0)	38 (92.7)	
2	0	3 (7.3)	--
Calcification, N (%)			
1	56 (84.8)	33 (80.5)	
2	10 (15.2)	8 (19.5)	0.601
Obstructive changes, N (%)			
1	35 (53.0)	27 (65.9)	
2	30 (45.5)	12 (29.3)	
3	1 (1.5)	2 (4.9)	0.160
Involved vessel pattern, N (%)			
1	35 (53.0)	24 (58.5)	
2	6 (9.1)	6 (14.6)	
3	16 (24.2)	9 (21.9)	
NA	9 (13.6)	2 (4.9)	0.455
Nodules in the same lobe, N (%)			
1	57 (86.4)	31 (75.6)	
2	9 (13.6)	10 (24.4)	0.196
Nodules in other lobes, N (%)			
1	49 (74.2)	35 (85.4)	
2	17 (25.8)	6 (14.6)	0.228
Lymphadenopathy, N (%)			
1	50 (75.8)	18 (43.9)	
2	8 (12.1)	5 (12.2)	
3	8 (12.1)	18 (43.9)	**0.001**
Pleural nodules, N (%)			
1	56 (84.8)	35 (85.4)	
2	10 (15.2)	6 (14.6)	0.999
Mean longest dimension (cm), (SD)	3.38 (1.15)	3.92 (2.06)	0.085
Mean largest short dimension (cm), (SD)	2.60 (0.85)	2.97 (1.56)	0.121
Mean CT value pre-contrast (HU), (SD)	27.66 (9.95)	27.73 (11.39)	0.974
Mean CT value post-contrast (HU), (SD)	70.26 (18.64)	64.76 (22.15)	0.203
Mean contrast enhancement (HU), (SD)	42.30 (18.51)	37.36 (15.99)	0.188
Mean TDR, (SD)	0.21 (0.24)	0.09 (0.09)	**0.005**

Abbreviations: TDR, tumor shadow disappearance rate; GGO, ground-glass opacity

Bolded values indicate a statistically significant result

Table 4

Multivariable logistic regression analyses

Characteristic	Odds Ratio (95% CI)
Age, continuous	0.93 (0.89 – 0.98)
GGO, N (%)	
1	1.00 (Referent)
2	0.14 (0.03 – 0.67)
Lymphadenopathy, N (%)	
1 and 2	1.00 (Referent)
3	4.15 (1.49 – 11.60)

Abbreviations: GGO, ground-glass opacity; CI, confidence interval